

Article

Assessing Wheat Frost Risk with the Support of GIS: An Approach Coupling a Growing Season Meteorological Index and a Hybrid Fuzzy Neural Network Model

Yaojie Yue ^{1,2,*}, Yao Zhou ³, Jing'ai Wang ^{1,2} and Xinyue Ye ⁴

¹ School of Geography, Beijing Normal University, Beijing 100875, China; jwang@bnu.edu.cn

² State Key Laboratory of Earth Surface Processes and Resource Ecology, Beijing Normal University, Beijing 100875, China

³ Department of Geography, University of Florida, Gainesville, FL 32611, USA; yaozhou@ufl.edu

⁴ Department of Geography, Kent State University, Kent, OH 44242, USA; xye5@kent.edu

* Correspondence: yjyue@bnu.edu.cn; Tel.: +86-10-5880-7454 (ext. 1632); Fax: +86-10-5880-6955

Academic Editor: Marc A. Rosen

Received: 18 September 2016; Accepted: 2 December 2016; Published: 13 December 2016

Abstract: Crop frost, one kind of agro-meteorological disaster, often causes significant loss to agriculture. Thus, evaluating the risk of wheat frost aids scientific response to such disasters, which will ultimately promote food security. Therefore, this paper aims to propose an integrated risk assessment model of wheat frost, based on meteorological data and a hybrid fuzzy neural network model, taking China as an example. With the support of a geographic information system (GIS), a comprehensive method was put forward. Firstly, threshold temperatures of wheat frost at three growth stages were proposed, referring to phenology in different wheat growing areas and the meteorological standard of *Degree of Crop Frost Damage* (QX/T 88-2008). Secondly, a vulnerability curve illustrating the relationship between frost hazard intensity and wheat yield loss was worked out using hybrid fuzzy neural network model. Finally, the wheat frost risk was assessed in China. Results show that our proposed threshold temperatures are more suitable than using 0 °C in revealing the spatial pattern of frost occurrence, and hybrid fuzzy neural network model can further improve the accuracy of the vulnerability curve of wheat subject to frost with limited historical hazard records. Both these advantages ensure the precision of wheat frost risk assessment. In China, frost widely distributes in 85.00% of the total winter wheat planting area, but mainly to the north of 35°N; the southern boundary of wheat frost has moved northward, potentially because of the warming climate. There is a significant trend that suggests high risk areas will enlarge and gradually expand to the south, with the risk levels increasing from a return period of 2 years to 20 years. Among all wheat frost risk levels, the regions with loss rate ranges from 35.00% to 45.00% account for the largest area proportion, ranging from 58.60% to 63.27%. We argue that for wheat and other frost-affected crops, it is necessary to take the risk level, physical exposure, and growth stages of crops into consideration together for frost disaster risk prevention planning.

Keywords: frost disaster; risk assessment; vulnerability curve; wheat; growth stage; threshold temperature; information diffusion; hybrid fuzzy neural network model; China

1. Introduction

Among weather risks, frost is responsible for serious agricultural production losses [1]. Although some areas have observed a reduction of frost days in recent years due to global warming [2–5], plant ecologists are concerned about a seemingly paradoxical relationship between plant growth and

climate change, which shows that a warming climate may actually increase the risk of plant frost damage [6], because fluctuations in spring temperatures are a real threat to terrestrial ecosystems' structure and function in a warming climate. Previous studies noticed that a warming climate may increase the risk of frost damage to plants in temperate regions [6,7]. Therefore, in the context of global warming, quantification of frost risk is very important in understanding the extent of risk and planning for its effective mitigation [8]. Thus, there is an urgent need to strengthen the study of frost disaster risk assessment.

Frost often occurs around the beginning of spring and the end of autumn, when cold air invades suddenly or there is a radiative cooling of the earth's surface [9–13]. The magnitude of freeze damage depends on the freezing temperatures, in combination with plant growth stages [11–13]. Thus, previous studies have taken low temperature indicators to estimate frost hazard [14], including daily minimum temperature [15–17] and the daily minimum temperature at the 850 hPa level in some areas [1]. Although it is assumed that frost is prone to occur once daily minimum temperatures fall below 2 °C [18,19], a 0 °C threshold of daily minimum temperature is accepted in most frost risk assessments. If the minimum temperature falls below 0 °C on any day during the growing period of plants in a certain year, the plant is assumed to have received frost injury during that year [5]. This threshold is adopted by numerous studies to explain major recent incidences of frost damage [20–26]. More specifically, daily values of minimum temperature ranges of 0 to –1.1 °C, –1.2 to –2.2 °C, and below –2.2 °C are considered to constitute mild, moderate, and severe frost intensities, respectively [27]. Zhong et al. [28] used temperature thresholds of 0 °C and –1.4 °C to indicate different probabilities of regions receiving frost injury.

Although minimum temperature has been widely used in frost risk research, few studies consider that different plants at different growth stages have different tolerance to low temperature, which also determines the damage or loss caused by frost [29,30]. As these studies mostly ignore the different tolerance to low temperature of different plants, their results cannot reveal the accurate risk level of different plants. Accurate frost risk assessment of different plants is needed to provide a scientific basis for the precise formulation of frost disaster prevention strategies. It is necessary to evaluate the frost risk by establishing the temperature thresholds based on the resistance of the plants to low temperature in different growth stages. On the other hand, vulnerable plants, as risk receptors, play a key role in determining the losses caused by frost. Vulnerability, which is defined as the degree to which a system is susceptible to and unable to cope with the adverse effects of climate change [31], is one of the key scientific issues in disaster risk assessment [32–35]. It is recognized as a propensity to suffer adverse consequences when crops are threatened [31,36–39]. However, most previous frost risk assessment did not take the plant's vulnerability into consideration. From this point, previous frost risk assessments remain at the stage of frost hazard assessment, instead of real risk assessment, therefore they cannot give any information on the loss of plants that were exposed to low temperatures.

Frost, as one of the major agro-meteorological disasters in China, affects crops including winter wheat, cotton, corn, rice, sorghum, fruits, and vegetables, and often causes a significant loss of agricultural income [5,40–42]. As the world's third largest wheat-producing country, China's wheat accounts for 30% of its total grain area, so frost injury to wheat can be particularly destructive and result in food insecurity [43–45]. Wheat ears, especially, can suffer severe frost damage with a reduced number of grains and sometimes the death of entire ears, if they are exposed to freezing temperature after heading [46]. In regions receiving serious frost in China, the area of wheat that was frozen to death in the immature ear period accounted for 97% of the total area of wheat fields and in some regions yield was reduced by 60% to 70% [44]. Moreover, frost hazards have increased in China since the 1990s. According to data from the Shangqiu meteorological station, the probability of wheat frost per year was close to 40% in the 1970s, 50% in the 1980s, and increased to 78% in the 1990s [47]. Yan et al. [48] found that the frequency of later frost occurring in the 1990s was 1.88 times higher than in the 1980s, although the number of years with warmer winters in the 1990s was twice that of the 1980s. China, as the most populous country with rapid economic growth, suffers great food insecurity

due to frost. Thus, a study on wheat frost risk assessment in China not only provides crucial scientific support for frost risk management, but also, ultimately, benefits China and the world's food security under a warming climate.

This paper, therefore, taking China as an example, attempts to explore the assessment methods of wheat frost risk, taking hazardous low temperatures and vulnerable plants into account, by combining threshold temperatures, winter wheat growth stages, and the hybrid fuzzy neural network model, with the support of GIS. By showing the process and results of the China case through implementing the proposed approach, the paper tries to test the feasibility of these methods and provide new thinking for frost risk research in specific areas.

2. Materials and Methods

2.1. Data Sources

Datasets of meteorology, historical disaster data of wheat, land use, wheat planting division, and wheat phenological phases were applied in this study. Meteorological data, including daily maximum and minimum temperature, wind speed, humidity, and precipitation, were obtained from 752 meteorological stations throughout China for the period from January 1966 to December 2005. Historical disaster data for wheat were obtained from the agro-meteorological station observations for January 1978 to December 2005, and from the *Encyclopedia of Meteorological Disasters in China* (records for every province from 1950 to 2000). The fields of the database include the province name, county code, weather station code, county name, year, month, day, the lowest temperature in the day or month affected by frost, and the production loss rate of in the affected year. Land use data (provided by the Data Center for Resources and Environmental Sciences of the Chinese Academy of Sciences, 2001, 1:1,000,000) were acquired from TM/ETM images during 1999–2000, whose average classification accuracy is about 81%, which can meet the requirements of researchers on the national scale [49,50]. The wheat planting division map (1:40,000,000) and the wheat phenological phase diagram were obtained from the National Agricultural Atlas of the People's Republic of China [51]. The wheat phenological phase diagram is composed of four maps (1:40,000,000) including the sowing period, the jointing period, the flowering period, and the harvest period. In this paper, the sowing period and the jointing period were integrated into the seedling stage.

Data processing, frost risk assessment, and results analysis were done on the ArcGIS platform. The meteorological station data were converted from dot into grid using the Inverse Distance Weighting (IDW) interpolation method. All the non-irrigated farmland in the national land use map was extracted as potential wheat-growing areas. A distribution map of the wheat planting was obtained by overlaying the potential wheat grow areas and the wheat planting division map. All the data were converted or re-sampled into a 1-km grid and registered to the Universal Transverse Mercator (UTM) projection with a WGS84-coordinate system.

2.2. Research Framework for Assessing Wheat Frost Risk

It is widely accepted that disaster risk can be defined as the probability of harmful impacts, or expected losses resulting from interactions between natural or human-induced hazards and vulnerable exposed elements [37,52]. Other researchers defined disaster risk as a function of three factors: hazard, vulnerability, and exposure [53,54]. We argue that exposure is an important property of the hazard-affected body in agricultural disaster risk assessment [55]. For wheat, its exposure covers the spatial distribution of planting and temporal distribution of growth. We therefore adopted the conceptual model proposed by Dilley et al. [54] to assess wheat frost risk:

$$R = H \times V \times E, \quad (1)$$

where R represents the frost disaster risk of wheat; H is the frost hazard index; V is the vulnerability of wheat to frost; and E is the exposure to frost, which refers to wheat being exposed to the effects of

low temperature. We assume that the wheat planting areas are dry farmland in a wheat planting zone. Then, E is assigned a value of 1 where there is wheat planted; otherwise E is 0.

Therefore, there are two key steps assessing the risk of wheat subjected to frost: (1) hazard assessment of frost based on threshold temperatures agreeing with the wheat growth stages; (2) vulnerability assessment of wheat using the hybrid fuzzy neural network model.

2.3. Hazard Assessment of Wheat Frost Risk

2.3.1. Threshold Temperature of Wheat Frost Hazard

The basic idea [56] for determining the threshold temperature of wheat frost hazard is to determine the start and end dates of the seedling stage, flowering stage, and harvest stage of wheat firstly, according to phenology in different wheat growing areas. Then, combined with the meteorological standard of frost in each growing stage, the threshold temperature of wheat frost was selected from meteorological data.

According to phenological phases of wheat, the start and end dates of three growth stages (Table 1), the seeding stage, the flowering stage, and the harvest stage, were acquired from the National Agricultural Atlas of the People's Republic of China [51].

Table 1. Wheat growth stages.

Wheat Planting Regions	Seedling Stage (mm/dd)	Flowering Stage (mm/dd)	Harvest Stage (mm/dd)
Beijing, Tianjin, Hebei, Shanxi	9/21–4/20	4/21–5/20	5/21–6/11
Shandong, Shannxi	10/1–3/31	4/1–4/30	5/1–6/11
Henan	10/11–3/20	3/21–4/20	4/21–6/11
Anhui, Jiangsu	10/21–3/10	3/11–4/20	4/21–6/1
Shanghai	10/21–2/29	3/1–4/20	4/21–6/1
Guizhou	10/21–2/10	2/11–3/20	3/21–5/21
Chongqing	11/1–1/20	1/21–2/29	3/1–5/1
Hubei	11/1–2/29	3/1–4/10	4/11–6/1
Hunan	11/1–2/20	2/21–3/31	4/1–5/21
Jiangxi	11/1–2/10	2/11–3/31	4/1–5/11
Sichuan	11/1–1/31	2/1–3/10	3/11–5/11
Yunnan	11/1–1/31	2/1–2/29	3/1–5/1
Zhejiang	11/11–2/20	2/21–4/10	4/11–5/11
Fujian	11/11–1/31	2/1–2/29	3/1–5/11
Guangdong, Guangxi	11/11–12/31	1/1–1/31	2/1–4/1
Liaoning	9/11–4/30	5/1–5/31	6/1–7/11
Gansu	9/11–4/30	5/1–5/31	6/1–7/21
Ningxia	9/21–4/30	5/1–5/31	6/1–7/11
Xinjiang	9/11–4/30	5/1–5/31	6/1–7/11
Tibet	9/11–5/10	5/11–6/10	6/11–9/1

Then, referring to the meteorological standard of the People's Republic of China "Degree of Crop Frost Damage (QX/T 88-2008)" [57], the threshold temperatures of three grades of frost damages at seedling stage, flowering stage, and harvest stage (based on the daily minimum air temperature, °C) of wheat were constructed (Table 2). A hazard assessment database was thus established by calculating the number of days of the spring frost and fall frost.

Table 2. Threshold temperatures of wheat frost (based on daily minimum temperature, °C).

Light Frost			Moderate Frost			Heavy Frost		
Seedling Stage	Flowering Stage	Harvest Stage	Seedling Stage	Flowering Stage	Harvest Stage	Seedling Stage	Flowering Stage	Harvest Stage
–7.0–8.0	0.0–1.0	–1.0–2.0	–8.0–9.0	–1.0–2.0	–2.0–3.0	–9.0–10	–2.0–3.0	–3.0–4.0

2.3.2. Wheat Frost Hazard Assessment Method

An exceeding probability prediction method was adopted to assess wheat frost hazard, based on the average daily minimum temperature in the wheat growing period, obtained according to the threshold temperatures of wheat frost (Table 2). The principle of this method is as follows.

In a certain period of time $[t_1, t_2]$, if the probability that the frost hazard intensity is equal to or more than S is defined as P and the cumulative probability is $CF(S)$, then the relationship between the probability of exceeding probability, hereafter denoted as $P(S)$, and the cumulative probability is as follows:

$$P(S) = \frac{CF(S)}{T}, \quad (2)$$

where T is the length of time period $[t_1, t_2]$; its value equals to $t_2 - t_1 + 1$. In this case, the time period is from 1966 to 2005, so $T = 40$.

During the period of time $[t_1, t_2]$, if the probability that the hazard intensity index is equal to or more than S is expressed by $P(S, t)$, then:

$$P(S, t) = 1 - \left[1 - \left(\frac{CF(S)}{T} \right) \right]^t = 1 - (1 - P(S))^t, \quad t \in [t_1, t_2]. \quad (3)$$

The probability of exceedance in every grid was calculated by using the average minimum temperature data in the growth period of wheat from 1966 to 2005, a total of 40 years. We ordered the average daily minimum temperature in descending order: if the rank of hazard intensity is 20, the intensity is defined as “once every 2 years”; if the rank of hazard intensity is 8, the intensity is defined as “once every 5 years”; if the rank of hazard intensity is 4, the intensity is defined as “once every 10 years”; if the rank of hazard intensity is 2, the intensity is defined as “once every 20 years”. In a fixed exceedance probability (a certain level of risk), this paper drew wheat frost hazard risk maps for the four hazard risk levels including “once every 2 years”, “once every 5 years”, “once every 10 years” and “once every 20 years”.

2.4. Vulnerability Assessment of Wheat Frost Risk

Vulnerability assessment of wheat aims to find the relationship between low temperature and the observed wheat yield, which can give valuable information when trying to estimate the probability of agriculture losses. One of the methods is to build a vulnerability curve. As a fine quantitative assessment method, a vulnerability curve expresses the quantitative relationship between the hazard intensity and the vulnerability of the hazard-affected body. Practically, a vulnerability curve is constructed by using historical disaster data and statistical analysis [35]. However, historical records of disaster losses are often insufficient and incompatible for using traditional statistical methods to build vulnerability curves [58]. To simulate nonlinear and complex relations from small samples, Huang [58–60] proposed the hybrid fuzzy neural network model by combining the information diffusion method and the backpropagation algorithm (BP) for neural network.

This model employs the information diffusion method (IDM) to construct fuzzy “if-then” rules as many as the given observations. Contradictory patterns are changed to be compatible for training a BP neural network effectively by using an information-diffusion-approximate-reasoning estimator (IDAR). Huang and Leung [58] utilized hybrid fuzzy neural network model to estimate the relationship between isoseismal area and earthquake magnitude. They found that the IDM can change the contradictory patterns from a limited number of historical seismic records into more compatible ones, which can effectively train the neural network with backpropagation algorithm to obtain the accurate relationship. The hybrid fuzzy neural network model has been widely used in many studies [59–64], which shows that this model can effectively resolve the problems related to contradictory patterns from small samples and improve the accuracy of risk assessments.

2.4.1. Diffuse Historical Records Using the Information Diffusion Method

In this paper, a hybrid fuzzy neural network model approach was adopted to assess the wheat vulnerability [58,61]. We employed daily minimum temperature as a frost hazard indicator on frost days that were collected from wheat frost hazard cases in wheat planting regions during 1951–2002 as input sampling X , and yield loss rate of wheat as output sampling Y (Table 3). We derived patterns from (x_i, y_i) , $X = \{x_1, x_2, \dots, x_{25}\} = \{-18, -0.8, \dots, -30.1\}$ and $Y = \{y_1, y_2, \dots, y_{25}\} = \{0.45, 0.2, \dots, 0.80\}$ by using the information diffusion method. The procedures of hybrid fuzzy neural network modeling are described as follows:

Let $X = \{X_1, X_2, \dots, X_n\}$ be a given sample with daily lowest temperature x and yield loss rate of wheat y , then the given sample set could be written as

$$X = \{X_1, X_2, \dots, X_n\} = \{(x_1, y_1), (x_2, y_2), \dots, (x_n, y_n)\}. \quad (4)$$

Then, let the discrete universe of discourse of daily lowest temperature be:

$$U = \{u_1, u_2, \dots, u_{62}\} = \{-30.6, -30.1, \dots, -0.1\},$$

where the step size is 0.5.

Let the discrete universe of discourse of yield loss rate of wheat be:

$$V = \{v_1, v_2, \dots, v_{20}\} = \{0.050, 0.100, \dots, 0.850\},$$

where the step size is 0.05.

We applied the equations from Huang and Leung [58] to obtain the normal diffusion coefficients for x and y as

$$h_x = 2.6851(b_x - a_x)/(25 - 1) = 3.3228 \quad \text{and} \quad h_y = 2.6851(b_y - a_y)/(25 - 1) = 0.0783.$$

$\mu(x_i, u)$ is assumed as the normal diffusion function of x_i in set U , and then normalized by maximum value to obtain $\mu_{x_i}(u)$. A fuzzy classification function is constructed by normal diffusion equations (5), which reflects the extent to which u belongs to the fuzzy set “ x_i near”.

$$\mu(x_i, u) = \frac{1}{h_x \sqrt{2\pi}} \exp \left[-\frac{(u - x_i)^2}{2h_x^2} \right] \quad (5)$$

$$\mu_{y_i}(y_i, v) = \frac{1}{h_y \sqrt{2\pi}} \exp \left[-\frac{(v - y_i)^2}{2h_y^2} \right]$$

Then any input–output observation such as $(x_i, y_i) \in X$ in Formula (3) can be transformed to two fuzzy sets:

$$A_i = \int_U \mu_{x_i}(u) / u, \quad B_i = \int_V \mu_{y_i}(v) / v. \quad (6)$$

Applying the normal information diffusion Equations (5) and (6), observation X_i can be changed into fuzzy subsets as

$$\mu_{R_i}(u, v) = \mu_{A_i}(u) \mu_{B_i}(v); u \in U, v \in V. \quad (7)$$

Thus, n fuzzy relation matrices can be obtained from n samples.

For example, let $i = 1$, then $(x_1, y_1) = (-18, 0.45)$, and the fuzzy subset is calculated as

$$R_1 = \begin{matrix} & & v_1 & \dots & v_7 & v_8 & v_9 & v_{10} & \dots & v_{15} \\ \begin{matrix} u_1 \\ \vdots \\ u_{22} \\ u_{23} \\ u_{24} \\ u_{25} \\ u_{26} \\ u_{27} \\ \vdots \\ u_{62} \end{matrix} & = & \begin{pmatrix} 0.000 & \dots & 0.000 & 0.000 & 0.000 & 0.000 & 0.000 & \dots & 0.000 \\ \dots & \dots \\ 0.000 & \dots & 0.394 & 0.726 & 0.891 & 0.726 & \dots & 0.000 \\ 0.000 & \dots & 0.419 & 0.772 & 0.947 & 0.772 & \dots & 0.000 \\ 0.000 & \dots & 0.435 & 0.802 & 0.984 & 0.802 & \dots & 0.000 \\ 0.000 & \dots & 0.442 & 0.815 & 0.999 & 0.815 & \dots & 0.000 \\ 0.000 & \dots & 0.439 & 0.810 & 0.993 & 0.810 & \dots & 0.000 \\ 0.000 & \dots & 0.467 & 0.786 & 0.964 & 0.786 & \dots & 0.000 \\ \dots & \dots \\ 0.000 & \dots & 0.000 & 0.000 & 0.000 & 0.000 & \dots & 0.000 \end{pmatrix} \end{matrix} .$$

In the actual calculation, U is usually not continuous, so x_0 is not equal to any value in U . Under this situation, a fuzzy set as input can be obtained by the information distribution equations (8):

$$\mu_{x_0}(u_j) = \begin{cases} 1 - |x_0 - u_j|/\Delta, & |x_0 - u_j| \leq \Delta \\ 0, & |x_0 - u_j| > \Delta \end{cases} , \tag{8}$$

where $\Delta = u_{j+1} - u_j$.

When the minimum temperature is given, suppose $x_0 = -18$, we can change it into a fuzzy subset of U by using the information distribution Equation (8) as follows:

$$\tilde{x} = \sum_{j=1}^{62} \mu_{x_0}(u_j)/u_j = 0/-30.600 + 0/-30.100 + \dots + 0.8/-18.1 + 0.2/-17.600 + \dots + 0/-0.1.$$

From the fuzzy set of x_0 and R_i to the fuzzy inference, the membership function is as follows:

$$\mu_{y_0}(v) = \sum_u \mu_{x_0}(u)\mu_{R_i}(u, v), \tag{9}$$

assuming

$$\mu_{y_0}(v') = \max\{\mu_{y_0}(v)\}. \tag{10}$$

Then the maximum non-diffused value $\hat{y}_i = v'$, and weight $w_i = \mu_{y_0}(v')$. Then the result is calculated by using an integration formula to combine all R_1, R_2, \dots, R_n :

$$\tilde{y}_0 = \left(\sum_{i=1}^n w_i \hat{y}_i \right) / \left(\sum_{i=1}^n w_i \right). \tag{11}$$

When given $x = -18$, the relevant output value \tilde{y}_1 is 0.445. This means that, in major wheat planting regions of China, according to historical frost loss records, if the daily minimum temperature reaches -18 degrees Celsius, the loss rate of winter wheat is about 44.5%. The model composed of the Equations (4)–(11) is the information diffusion approximate reasoning. Then the historical disaster records $((x_1, y_1), (x_2, y_2), \dots, (x_n, y_n))$ can be transformed to new samples $((x_1, \tilde{y}_1), (x_2, \tilde{y}_2), \dots, (x_n, \tilde{y}_n))$ by the information diffusion approximate reasoning.

2.4.2. Vulnerability Curving of Winter Wheat Based on Diffused Historical Disaster Data

The BP neural network has been widely used in disaster assessment and other relevant fields [58–61]. In this paper, we first employed the abovementioned information diffusion method to

get diffused derivative samples. Then the BP neural network was trained by the derivative samples on the Matlab platform to simulate the relationship between the minimum temperature and the yield loss rate of wheat. Lastly, a vulnerability curve was built by using the output of well-trained BP neural network and linear regression.

3. Results

3.1. Vulnerability Curve of Wheat Subjected to Frost

The diffused samples and the original samples are shown in Table 3. Each dataset was used to train a conventional BP neural network with one node in the input and output layer, respectively, and five nodes in the hidden layer. The BP neural network was trained by the original samples $X(x, y)$ and the diffused samples $\tilde{X}(x, \tilde{y})$, respectively. After 10,000 iterations, the normalized system errors are 0.00531 and 0.0001, respectively.

Table 3. The original sample data (y) and the diffused sample data (\tilde{y}).

Sample	1	2	3	4	5	6	7	8	9	10	11	12	13
x	-18	-0.8	-5.5	-6	-10	-4.6	-0.6	-9.9	-3.7	-8.8	-10.9	-3.7	-15
y	0.45	0.2	0.25	0.25	0.5	0.25	0.25	0.3	0.15	0.2	0.55	0.1	0.5
\tilde{y}	0.446	0.231	0.274	0.283	0.369	0.260	0.230	0.367	0.249	0.344	0.385	0.249	0.432
Sample	14	15	16	17	18	19	20	21	22	23	24	25	
x	-25.6	-11.6	-11	-3.8	-10.4	-10.9	-0.4	-6	-17.4	-2.2	-4.3	-30.1	
y	0.65	0.5	0.4	0.25	0.3	0.4	0.2	0.5	0.4	0.33	0.15	0.8	
\tilde{y}	0.671	0.396	0.386	0.250	0.376	0.385	0.23	0.283	0.443	0.237	0.256	0.757	

The performance of the BP neural network was tested using the values of the optimal regression line slope (m), the y -axis intercept (b), and the correlation coefficient (r). This showed that the values of m , b , and r using the original sample data (y) and the diffused sample data (\tilde{y}) are 0.8114 and 0.9151, 0.0666 and 0.0263, and 0.9008 and 0.9934, respectively. The mean square error (MSE) of input–output simulation is 0.1986 using diffused historical records, while it is 0.2133 using original records, which also indicates that the input–output relationship trained by the BP neural network using the diffused samples is much better and more stable than the conventional BP neural network. This suggests that the hybrid fuzzy neural network model approach could solve problems arising from insufficient and contradictory historical disaster data.

The relationship between the daily minimum temperature and the loss rate of winter wheat production is estimated (Figure 1). Both daily minimum temperature and the loss rate of winter wheat production are standardized in Figure 1. Finally, the vulnerability assessment model of wheat subjected to frost was worked out using Gaussian regression based on the output of the BP neural network (Equation (12)):

$$\begin{aligned}
 V = & 0.6037 \times e^{-\left(\frac{x-1.051}{0.2867}\right)^2} + 0.09799 \times e^{-\left(\frac{x-0.8276}{0.09197}\right)^2} \\
 & + 0.01931 \times e^{-\left(\frac{x-0.7628}{0.05842}\right)^2} + (5.758e + 012) \times e^{-\left(\frac{x+58.39}{10.51}\right)^2}, \quad (R^2 = 0.9981), \\
 & + 0.2882 \times e^{-\left(\frac{x-0.5277}{0.3395}\right)^2}
 \end{aligned}
 \tag{12}$$

where V is the loss rate of wheat subjected to frost hazard and x is the frost hazard intensity index.

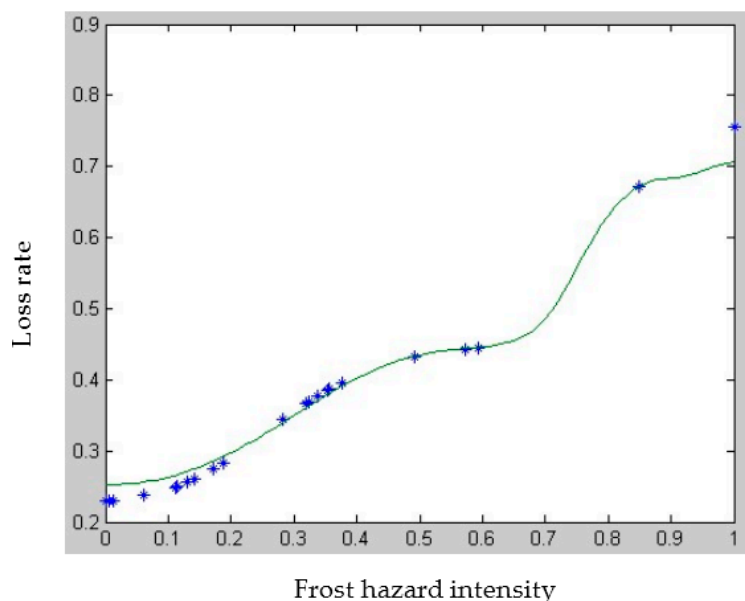


Figure 1. Vulnerability curve of wheat subjected to frost (data from Zhou et al., 2010 [64]).

3.2. Wheat Frost Days in China

The period of spring frosts of winter wheat ranges from 0 to 149 days; the distribution is shown in Figure 2. This indicates that the area affected by the spring frosts of winter wheat is about 85.00% of the land area in China. The area percentage of regions receiving spring frosts of winter wheat over 0–20 days, 20–40 days, 40–60 days, 60–80 days, and >80 days accounted for 40.00%, 10.00%, 16.00%, 20.00%, and 14.00%, respectively. The area where the days of the winter wheat spring frost are more than 60 stretch like a band along southern Inner Mongolia, northern Hebei Province, Beijing, Tianjin, northern Shanxi, and Shaanxi, finally directly to Ningxia. The “band” is divided into two parts in Gansu, one branch folding to the northwest along the Hexi Corridor and the other folding to southeastern Sichuan from northern Gansu and northwestern Sichuan.

The areas where the days of the spring frosts of winter wheat are more than 80 mainly distribute in northern Xinjiang and Tibet. It can be up to 149 days in the central region of Tibet. However, except for northern Xinjiang, where winter wheat is scattered, these regions do not belong to China’s winter wheat growing areas, so the actual loss caused by frost damage is less. The real danger regions are Liaoning, Hebei, Beijing, Tianjin, Shanxi, Shaanxi, Ningxia, Henan, and Shandong, which are the main growing areas for winter wheat in China and experience 20–80 frost days.

The days of the winter wheat fall frost range from 0 to 74, and the distribution has the similar band pattern (Figure 3). However, the distributed areas are smaller, mainly in 35°N–45°N. The area of winter wheat receiving 0–20, 20–40 and >40 days of fall frost accounts for 44.70%, 41.18% and 14.12% of total area, respectively. The areas with 0–40 frost days are mainly distributed in the southern part of Inner Mongolia, Liaoning, northern Hebei, Shanxi, northern Shaanxi, Ningxia, and Gansu Hexi Corridor. While, the areas with >40 days are still mainly distributed in northern Xinjiang and Tibet.

The spring frost days of spring wheat region range from 0 to 72, and the distribution is shown in Figure 4. The spring wheat areas with less than 40 spring frost days account for 86.66% of the total land area in China. Frost mainly distributes in the regions of Xinjiang, Tibet, central and southern Inner Mongolia, Heilongjiang, and Northern Inner Mongolia. Compared to winter wheat frost and spring wheat spring frost, the duration of spring wheat fall frost was much shorter; the highest was only 16 days. The spring wheat region impacted by fall frost is mainly distributed in the region west to 105°E, and 92.67% of these regions received more than five frost days. The number of frost days is relatively high in the Qinghai Tibet Plateau and Hexi corridor.

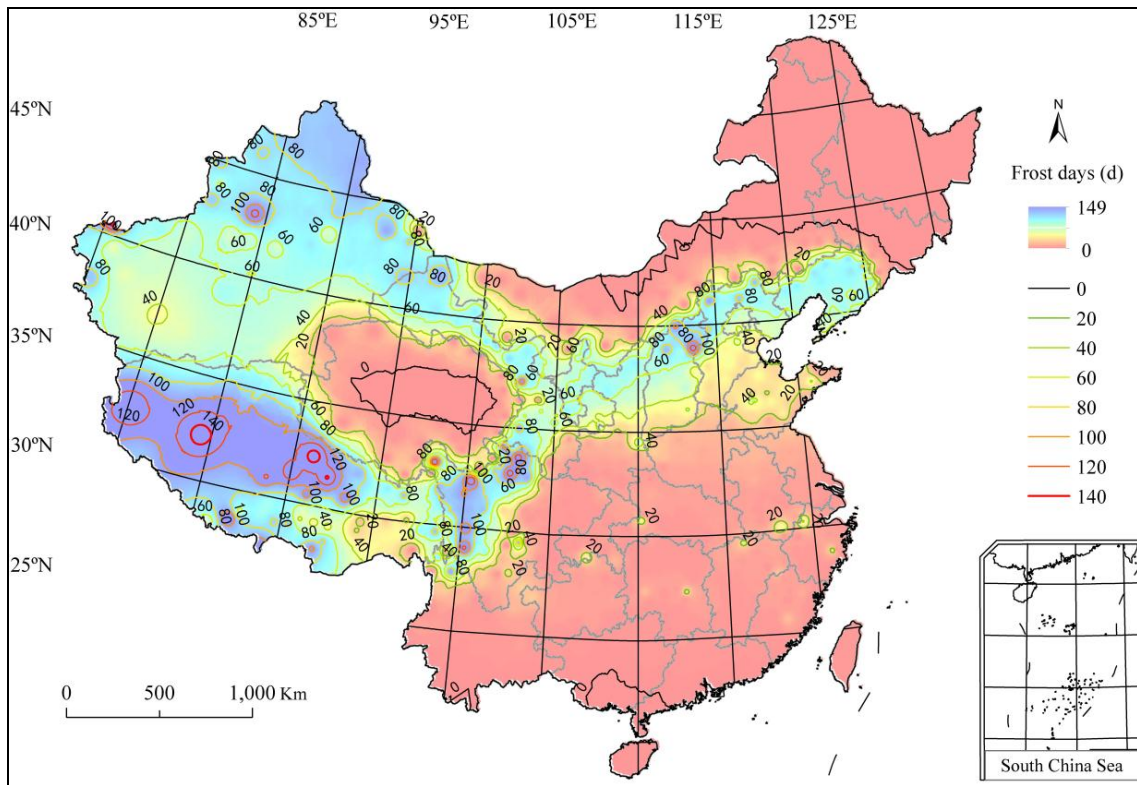


Figure 2. Winter wheat spring frost days in China.

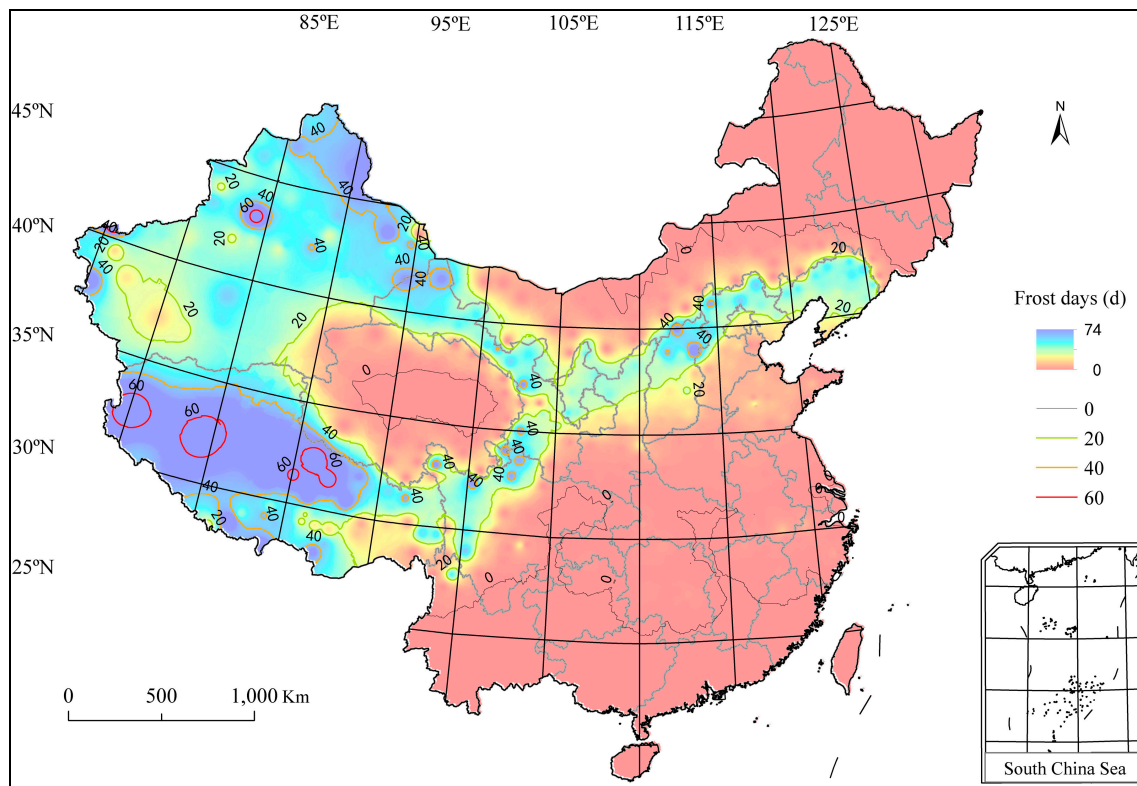


Figure 3. Winter wheat fall frost days in China.

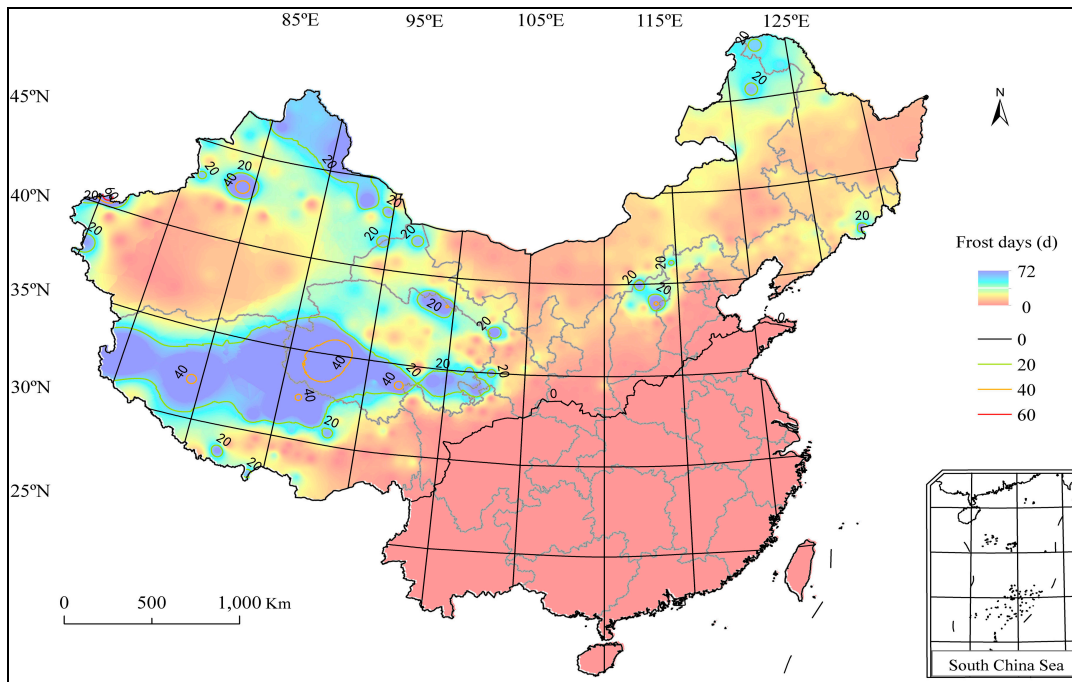
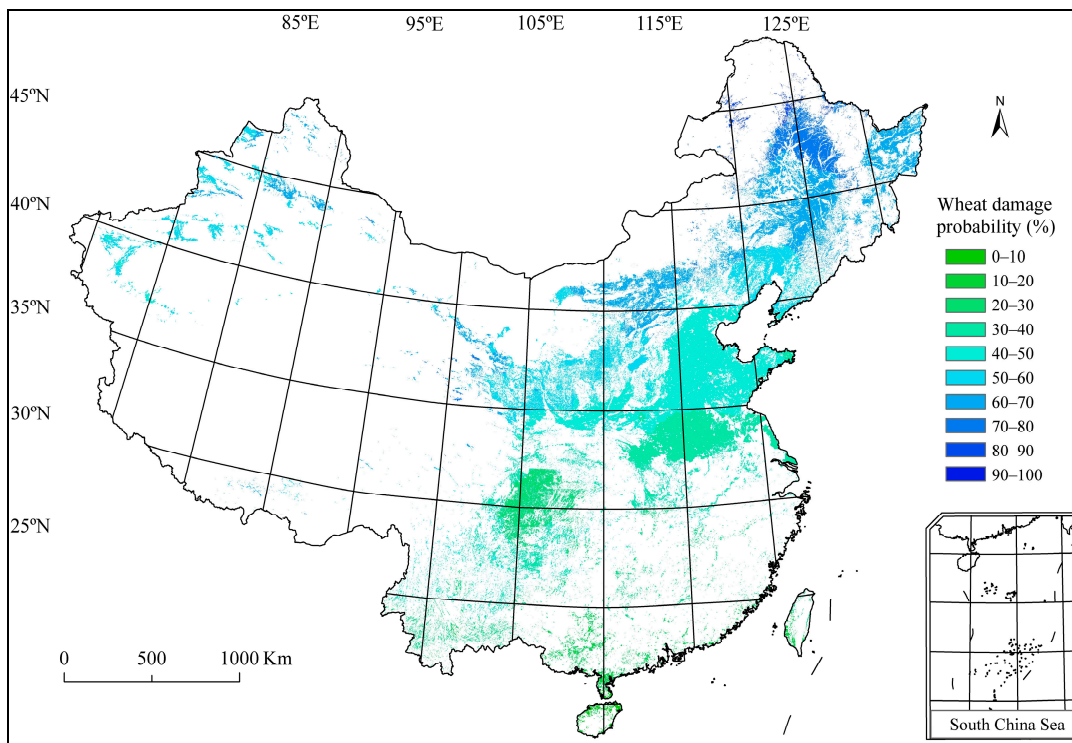


Figure 4. Spring wheat spring frost days in China.

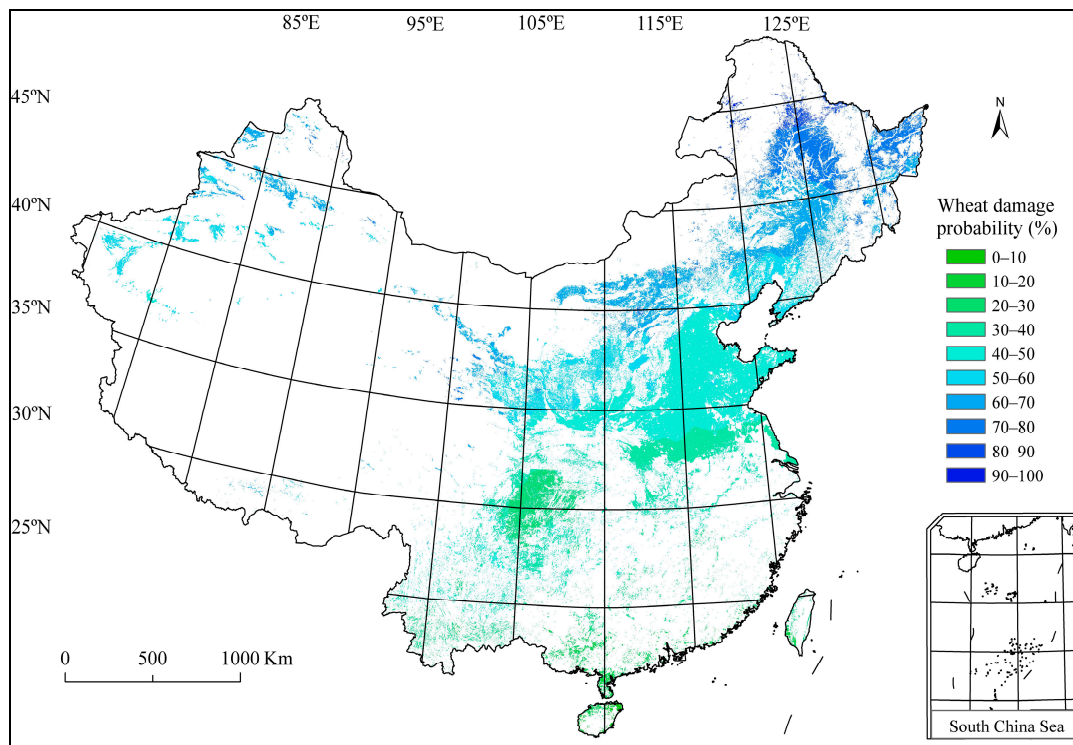
3.3. Wheat Frost Hazard in China

Distribution of wheat damage probability was subject to four frost hazard intensity levels in China, which were determined by four fixed exceedance probabilities (once every 2 years, once every 5 years, once every 10 years, and once every 20 years), as shown in Figure 5.

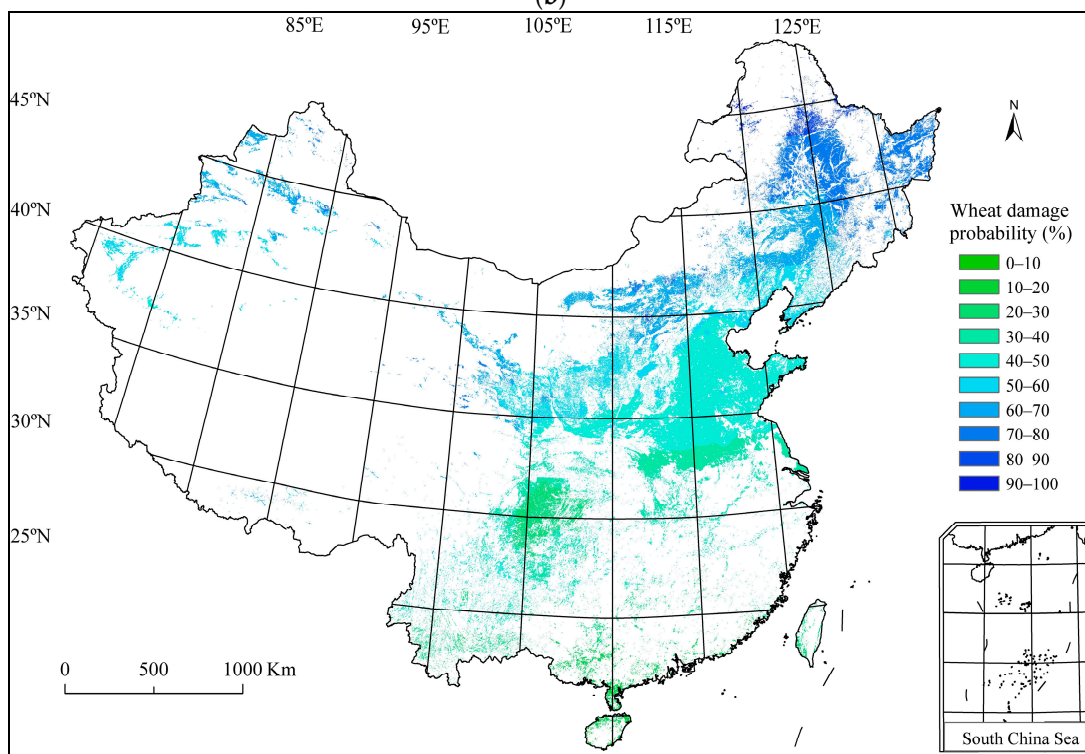


(a)

Figure 5. Cont.



(b)



(c)

Figure 5. Cont.

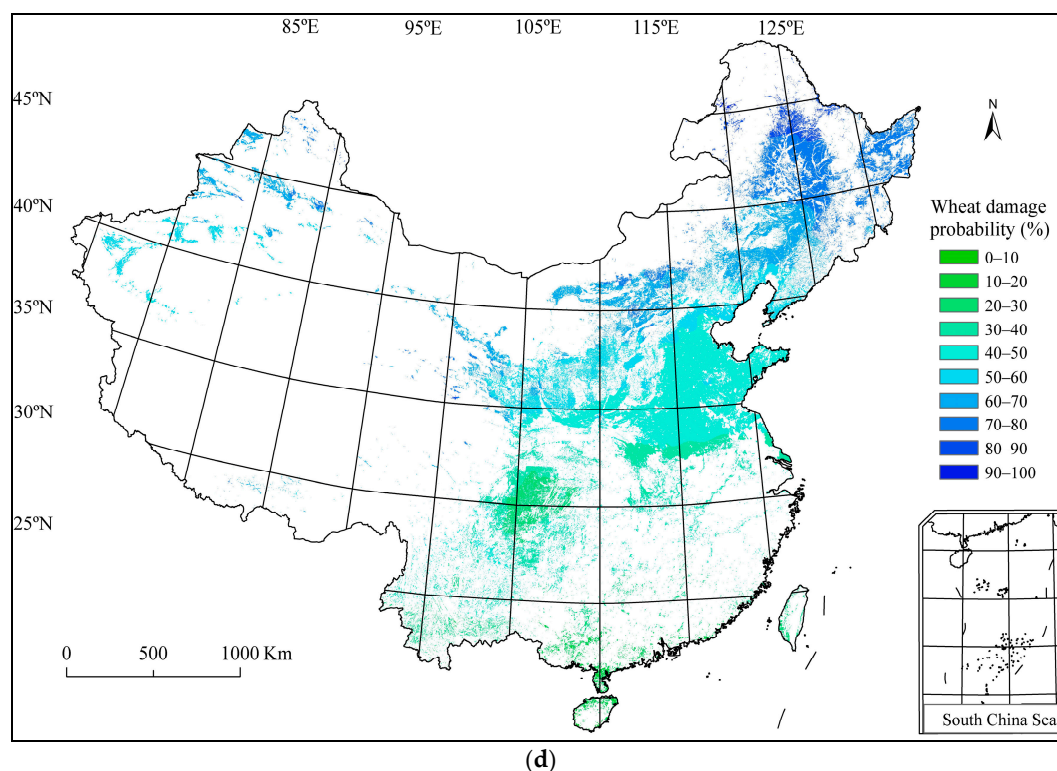


Figure 5. Distribution of wheat damage probability subjected to different frost hazard intensity levels in China (a) once every 2 years; (b) once every 5 years; (c) once every 10 years; (d) once every 20 years.

From those four maps, it can be seen that high-risk areas of wheat frost hazard are concentrated to the north of 35°N. The regions with the highest risk are in the northeast of China and Xinjiang Autonomous Region. With the frost intensity levels increasing from “once every 2 years” to “once every 20 years”, the high- and medium-risk regions extend towards the south of China. However, the wheat frost hazard intensity is relatively low in south China, generally. Area percentage of regions with different probability of wheat damage and frost intensity levels is shown in Table 4.

Table 4. Area percentage of regions with different wheat damage probability and frost intensity levels (%).

Probability	Frost Intensity Level			
	Once Every 2 Years	Once Every 5 Years	Once Every 10 Years	Once Every 20 Years
0.00–10.00	0.66	0.35	0.11	0.08
10.00–20.00	2.61	2.47	2.49	2.39
20.00–30.00	9.22	8.29	7.54	7.10
30.00–40.00	18.27	15.52	15.03	13.74
40.00–50.00	23.06	25.61	26.32	26.97
50.00–60.00	16.53	14.73	14.23	14.03
60.00–70.00	22.57	20.46	18.38	18.02
70.00–80.00	6.21	10.75	13.73	14.87
80.00–90.00	0.88	1.76	2.03	2.62
90.00–100.00	0.01	0.06	0.15	0.17

Regardless of the intensity levels of wheat frost, regions with wheat damage probability of 0.00%–10.00% occupy the smallest area, with an area ratio less than 1.00%. However, regions with wheat damage probability of 30.00%–70.00% account for 80.00% of the total area, which shows that wheat frost damage, may occur widely in China. Furthermore, the largest proportion of the area is that

with wheat damage probability of 40.00%–50.00%, ranging from 23.06% to 26.97% of all lands with wheat frost intensities of once every 2 years to once every 20 years. This further confirmed that no matter the intensity of wheat frost, nearly one-quarter of land has a 50% probability of frost damage to wheat, which means that the potential occurrence of wheat frost disaster is widely distributed in China.

3.4. Wheat Frost Risk in China

The wheat yield loss rate caused by frost was calculated according to Equation (1) based on frost hazard intensity and the vulnerability curve of wheat. Risk distribution maps, showing the loss rate under different wheat frost risk levels (once in 2 years, once in 5 years, once in 10 years, and once in 20 years), were drawn (Figure 6).

These results show that high frost risk areas of wheat (loss rate over 45.00%) in China mainly distribute to the north of 40°N and only a small part are located in Qinghai, Tibet, and Gansu. Regardless of the risk levels, the areas with the highest wheat loss rate subject to frost are mainly located in Heilongjiang Province. Then the areas with relatively high wheat frost risk lie between 40°N and 35°N, including Heilongjiang, Jilin, Liaoning, Inner Mongolia, and Xinjiang Autonomous Region. The wheat frost risk is relatively low in Yellow River Basin and Huaihe River Basin, and the lowest risky areas are Yangtze River Basin and Pearl River Basin. Among all the wheat planting regions, special attention should be paid to the Huang-Huai-Hai Plain. Although it is a major winter wheat planting area and produces the greatest portion of wheat in China, the loss rate is only moderate (from 35.00% to 45.00%). However, spring frost often produces a major loss of winter wheat yield in this area, since spring frost usually occurs at the ear stage, which is the most vulnerable growth stage of winter wheat. We therefore argue that, for wheat and even other frost-affected crops, it is necessary to consider frost risk level, physical exposure, and growth stages of crops together in frost risk prevention planning.

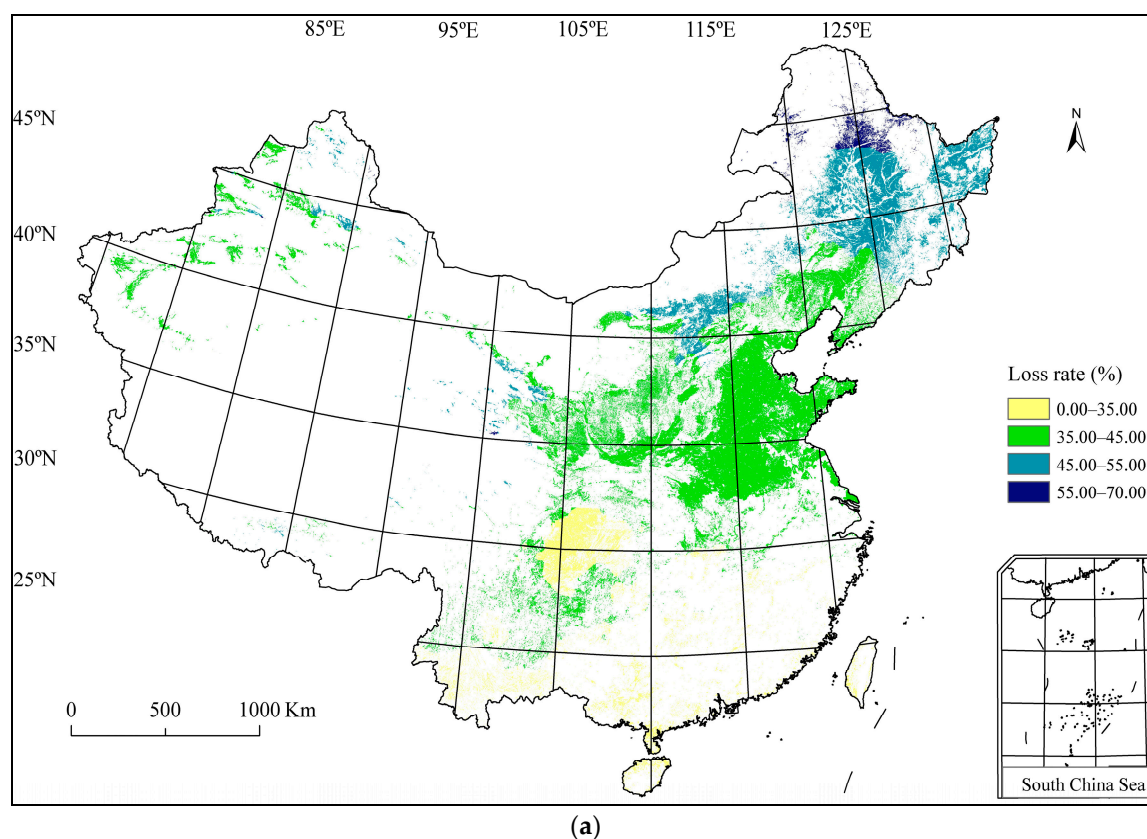
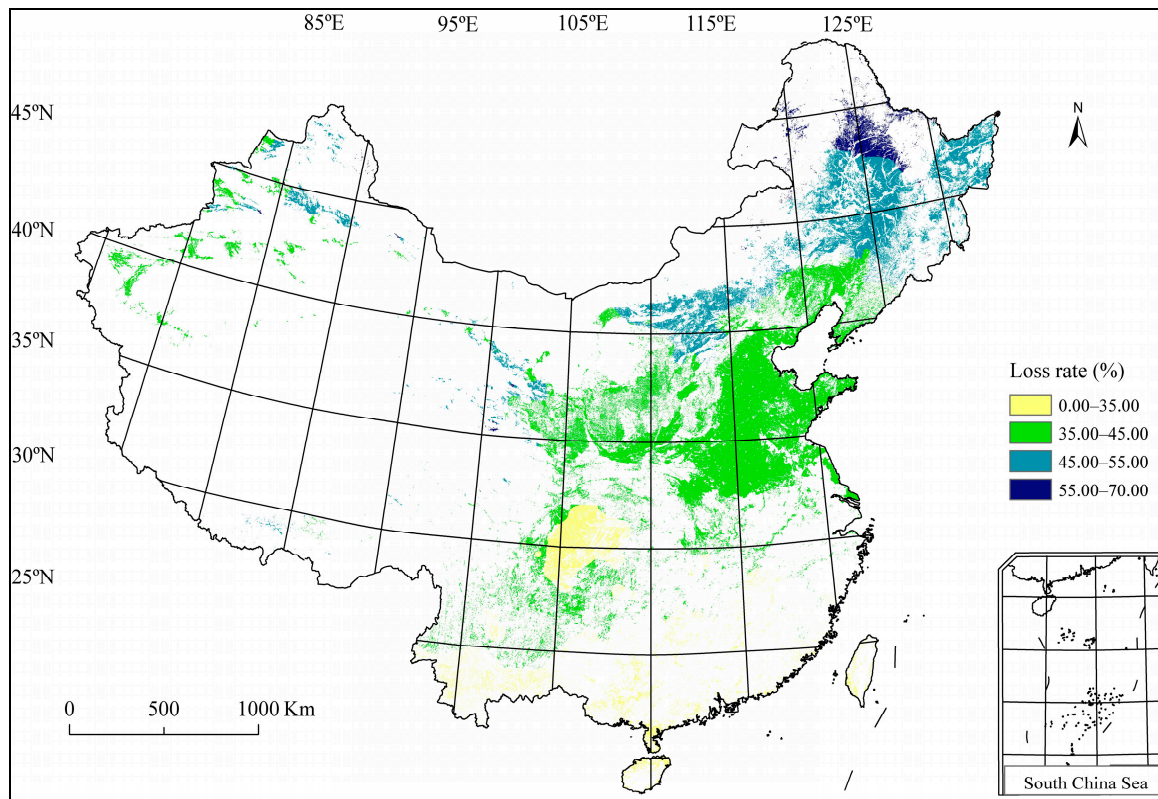
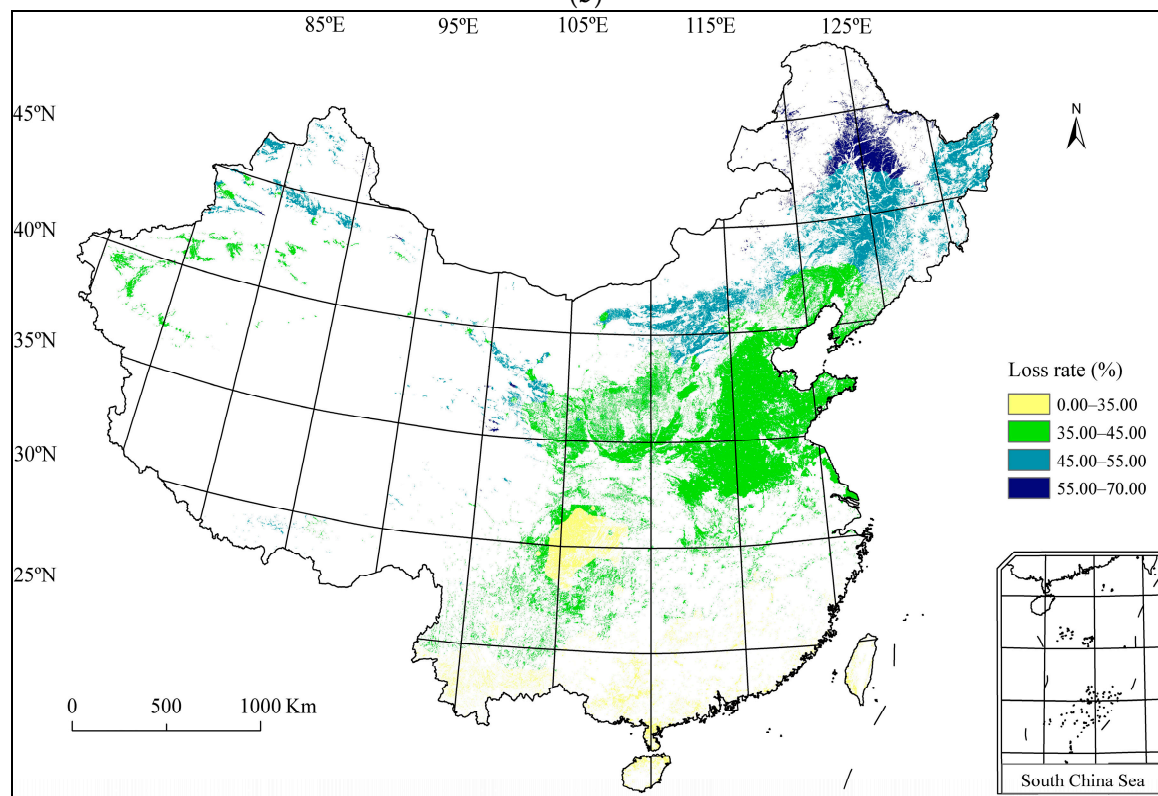


Figure 6. Cont.



(b)



(c)

Figure 6. Cont.

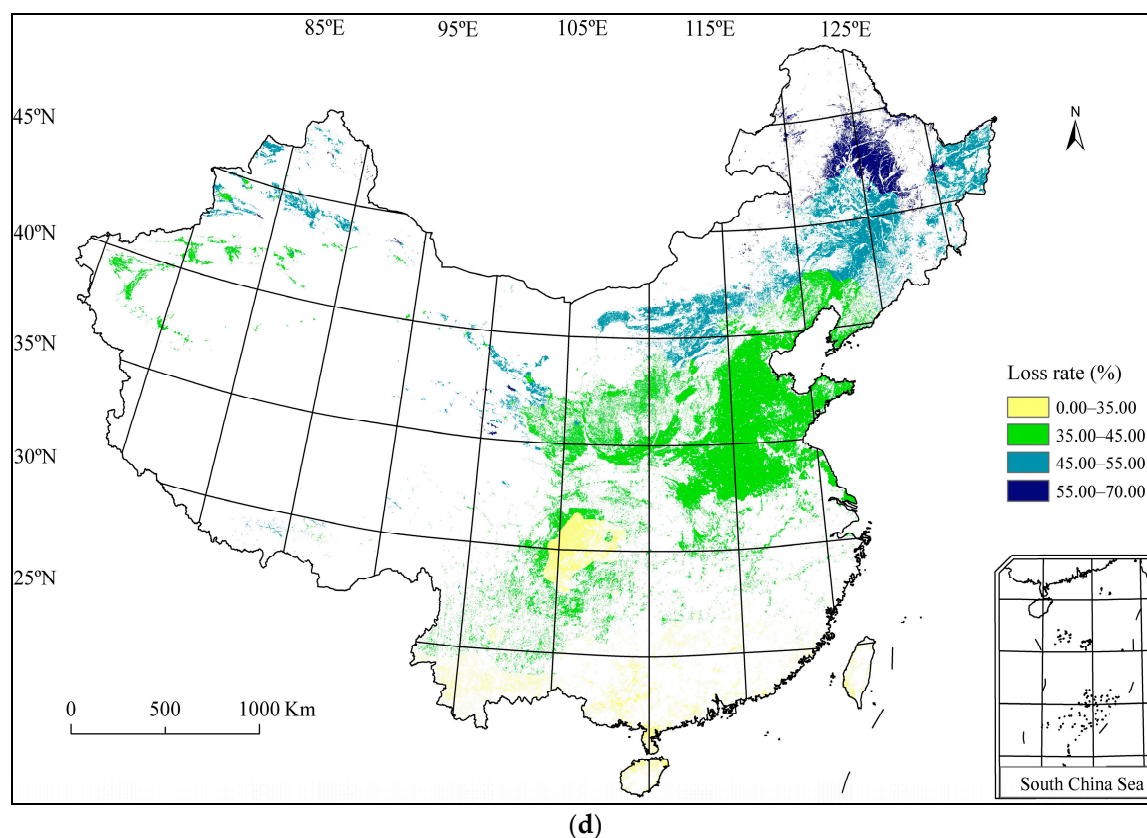


Figure 6. Wheat loss rate under different frost risk levels in China: (a) once every 2 years; (b) once every 5 years; (c) once every 10 years; (d) once every 20 years.

When the risk levels increase from a 2-year return period to a 20-year return period, the area with a wheat loss rate of 45.00%–55.00% or 55.00%–70.00% gradually increases (Table 5), and the southern boundary also gradually expands to the south (Figure 6). Among all wheat frost risk levels in China, the areas of loss rate from 35.00% to 45.00% account for the largest proportion of area, ranging from 58.60% to 63.27%. This indicates that most wheat planting areas face critical threats from frost. There is an urgent need to evaluate wheat frost risk under climate change so as to craft reasonable wheat frost risk prevention strategies for ensuring future food security.

Table 5. Area percentage of regions with different loss rate and different risk levels (%).

Loss Rate (%)	Risk Levels			
	Once Every 2 Years	Once Every 5 Years	Once Every 10 Years	Once Every 20 Years
0.00–35.00	12.64	11.21	10.31	9.71
35.00–45.00	63.27	60.71	59.54	58.60
45.00–55.00	21.34	23.73	24.11	24.18
55.00–70.00	2.75	4.35	6.04	7.51

4. Discussion

This paper proposed the threshold temperatures of wheat frost at three growth stages, referred to as the phenology in different wheat growing areas in the meteorological standard of *Degree of Crop Frost Damage* (QX/T 88-2008) [57], based on meteorological data. The threshold temperatures used by previous studies about frost risk assessment varied greatly, such as below 0 °C [20–26], 0 to −1.1 °C, −1.2 to −2.2 °C and below −2.2 °C [27], 0 °C, and less than −1.4 °C [28]. However, these threshold temperatures mostly blurred the differences in vegetation resistance to low temperature, which leads

to inaccurate risk assessment of different plants. On the contrary, our proposed threshold temperatures are conducive to high-precision wheat frost risk assessment and avoid the shortcomings of previous threshold temperatures. The results of wheat frost risk assessment using the proposed threshold temperatures will, therefore, be crucial for the precise formulation of frost disaster prevention strategies.

We argue that the vulnerability of plants plays a key role in frost risk formation [32–35], which we should take into account in frost risk assessment. Vulnerability is recognized as a propensity to suffer adverse consequence of when crops are threatened [36–39]. However, one of the difficulties of assessing wheat's vulnerability to frost is a shortage of historical records of wheat yield loss under the threat of low temperatures. To solve this problem, a hybrid fuzzy neural network model combining the information diffusion method and the BP neural network was adopted to produce a vulnerability curve of wheat subjected to frost. The results indicate that hybrid fuzzy neural network model could solve the problems arising from limited frost disaster records by diffusing the valid data. In comparison with previous studies [65–67], the introduction of the vulnerability curve makes it possible to quantitatively evaluate the risk of wheat yield loss due to frost hazard. Furthermore, this method is expected to improve the accuracy of the wheat vulnerability curve, if there are adequate frost disaster data.

The spatial pattern of frost days, hazard intensity and the risk levels of wheat frost disaster in China were successfully revealed by applying the proposed methods. Using the minimum temperature on a frost day as the index, Feng et al. [44] pointed out that wheat frost is mainly distributed in the range of 105°E–120°E and 33°N–38°N. However, our results indicate that it is mainly distributed to the north of 35°N. There may be two reasons for this difference. Firstly, although both Feng et al.'s and our study used the daily minimum temperature as the frost index, the threshold temperatures of frost hazard applied in our study were further improved by combining growth stages of wheat. Therefore, the frost days and area of impacted region in our study are less than results from Feng et al., but our results are more accurate. On the other hand, the southern boundary of wheat frost moved northward, implying that global warming potentially had a tremendous impact on the spatial distribution of frost. For example, a decreased trend of frost days has been observed in China [5].

Although a yield reduction of 60.00%–70.00% in the most seriously affected regions has been reported [44], such a serious wheat frost does not occur frequently. Our findings show that among all wheat frost risk levels in China, the areas with a loss rate between 35.00% and 45.00% account for the largest proportion of area, ranging from 58.60% to 63.27%. However, these results remind us that the risk of wheat frost is still very serious in China. Among all the wheat-planting zones, more attention should be paid to the Huang-Huai-Hai winter wheat planting region (110°E–118°N and 34°N–36°N), which produces the most wheat in China and is regarded as the area hardest hit by frost [44], with an increasing probability of wheat frost since the 1970s [47,48]. In this region, global warming may lead to advanced growth in the jointing stage and ear stage, accompanied by a strong alternating cold and warm climate, which may actually increase the risk of frost damage to plants in temperate regions [6,7,9,10]. For example, wheat ears can suffer severe frost damage, with a reduced number of grains and sometimes the death of entire ears when exposed to freezing temperature after heading [46]. We therefore argue that, for wheat and other frost-affected crops, it is necessary to consider the risk level, physical exposure, and growth stages of crops together in disaster risk prevention planning [55]. Moreover, in the context of global climate change, research on the impact of global warming on crop frost risk needs to be strengthened.

5. Conclusions

Evaluating the risk of wheat frost will aid the scientific response to such disasters and ultimately promote food security. In this paper, frost days and daily minimum temperature data were extracted according to wheat growth periods. A vulnerability curve for wheat subject to frost was built based on data of historical disasters using the hybrid fuzzy neural network model. The wheat frost risk in China was assessed. The conclusions are as follows:

The proposed methodology, coupling the wheat growing season meteorological frost index with a hybrid fuzzy neural network model, has been shown to improve the accuracy of wheat frost risk assessment, which is conducive to an accurate understanding of the patterns of wheat frost risk. The proposed threshold temperatures are conducive to high-precision wheat frost risk assessment, avoiding the shortcomings of previous threshold temperatures. The results indicate that the hybrid fuzzy neural network model could solve problems arising from limited frost disaster records by diffusing the valid data. Furthermore, this approach is expected to improve the accuracy of the wheat vulnerability curve, if there are adequate frost disaster data.

The spatial pattern of frost days, hazard intensity, and the risk levels of wheat frost disaster in China were successfully revealed by applying the proposed methods. Among all frost disaster risk levels of wheat in China by return period, the area of 2-year return period is the largest, accounting for 63.27%. Among all wheat frost risk levels, the areas where the loss rate ranges from 35.00% to 45.00% account for the largest proportion of area, ranging from 58.60% to 63.27%. Wheat frost mainly distributes to the north of 35°N and high-risk wheat areas mainly lie to the north of 40°N. From a 2-year return period to a 20-year return period, the area of high and moderate risk increases gradually, and high- and moderate-risk areas expand to the south. Wheat frost risk is relatively low in Yangtze River Basin and Pearl River Basin.

The wheat frost risk is still very serious and should receive more attention, especially in the Huang-Huai-Hai winter wheat planting region. It is observed that the southern boundary of wheat frost moved northward, potentially because of the warming climate. However, global warming may also lead to increased risk of frost damage to plants in temperate regions. Therefore, research on the impact of global warming on crop frost risk needs to be strengthened.

Acknowledgments: This research was financially supported by the National Key Research and Development Program of China (No. 2016YFA0602402), the National Natural Science Foundation of China (No. 41271515), and the Chinese Ministry of Education (No. 13JJD790008).

Author Contributions: Yaojie Yue designed the research; Yao Zhou and Yaojie Yue performed the research; Yaojie Yue and Yao Zhou wrote the paper; Jing'ai Wang co-designed the research; Xinyue Ye extensively updated the paper. All authors read and approved the final manuscript.

Conflicts of Interest: The authors declare no conflict of interest.

References

1. Papagiannaki, K.; Lagouvardos, K.; Kotroni, V.; Papagiannakis, G. Agricultural losses related to frost events: Use of the 850 hPa level temperature as an explanatory variable of the damage cost. *Nat. Hazards Earth Syst. Sci.* **2014**, *14*, 2375–2386. [[CrossRef](#)]
2. Heino, R.; Brázdil, R.; Førland, E.; Tuomenvirta, H.; Alexandersson, H.; Beniston, M.; Pfister, C.; Rebetez, M.; Rosenhagen, G.; Rösner, S.; et al. Progress in the study of climate extremes in northern and central Europe. *Clim. Chang.* **1999**, *42*, 151–181. [[CrossRef](#)]
3. Bonsal, B.R.; Zhang, X.; Vincent, L.A.; Hogg, W.D. Characteristics of daily and extreme temperature over Canada. *J. Clim.* **2001**, *14*, 1959–1976. [[CrossRef](#)]
4. Easterling, D.R. Recent changes in frost days and the frost-free season in the United States. *Bull. Am. Meteorol. Soc.* **2002**, *83*, 1327–1332.
5. Dai, J.H.; Wang, H.J.; Ge, Q.S. The decreasing spring frost risks during the flowering period for woody plants in temperate area of eastern China over past 50 years. *J. Geogr. Sci.* **2013**, *23*, 641–652. [[CrossRef](#)]
6. Gu, L.; Hanson, P.J.; Mac, P.W.; Kaiser, D.P.; Yang, B.; Nemani, R.; Pallardy, S.G.; Meyers, T. The 2007 eastern US spring freezes: Increased cold damage in a warming world? *Bioscience* **2008**, *58*, 253–262. [[CrossRef](#)]
7. Cannell, M.G.R.; Smith, R.I. Climatic warming, spring budburst and frost damage on trees. *J. Appl. Ecol.* **1986**, *23*, 177–191. [[CrossRef](#)]
8. Gobin, A.; Tarquis, A.M.; Dalezios, N.R. Preface “Weather related hazards and risks in agriculture”. *Nat. Hazards Earth Syst. Sci.* **2013**, *13*, 2599–2603. [[CrossRef](#)]

9. Li, M.S.; Wang, D.L.; Zhang, Q.; Chi, Y.G.; Wang, C.Y.; Kiribuchi-Otobe, C.; Yoshida, H. Cause analysis of frost damage to winter wheat in Huang-Huai-Hai plain during 2004–2005. *J. Nat. Disasters* **2005**, *14*, 51–55. (In Chinese with English abstract)
10. Li, M.S.; Wang, D.L.; Zhong, X.L.; Wang, C.Y.; Su, C.H.; Zhao, P.; Yan, X.Y.; Kiribuchi-Otobe, C.; Yoshida, H. Current situation and prospect of research on frost of winter wheat. *J. Nat. Disasters* **2005**, *14*, 72–78. (In Chinese with English abstract)
11. Eccel, E.; Rea, R.; Caffarra, A.; Crisci, A. Risk of spring frost to apple production under future climate scenarios: The role of phenological acclimation. *Int. J. Biometeorol.* **2009**, *53*, 273–286. [[CrossRef](#)] [[PubMed](#)]
12. Rigby, J.R.; Porporato, A. Spring frost risk in a changing climate. *Geophys. Res. Lett.* **2008**. [[CrossRef](#)]
13. Rodrigo, J. Spring frosts in deciduous fruit trees—Morphological damage and flower hardiness. *Sci. Hortic.* **2000**, *85*, 155–173. [[CrossRef](#)]
14. Varazanashvili, O.; Tsereteli, N.; Amiranashvili, A.; Tsereteli, E.; Elizbarashvili, E.; Dolidze, J.; Qaldani, L.; Saluqvadze, M.; Adamia, S.; Arevadze, N.; et al. Vulnerability, hazards and multiple risk assessment for Georgia. *Nat. Hazards* **2012**, *64*, 2021–2056. [[CrossRef](#)]
15. Laughlin, G.P.; Kalma, J.D. Frost Risk Mapping for Landscape Planning—A Methodology. *Theor. Appl. Climatol.* **1990**, *42*, 41–51. [[CrossRef](#)]
16. Zinoni, F.; Antolini, G.; Campisi, T.; Marletto, V.; Rossi, F. Characterisation of Emilia-Romagna region in relation with late frost risk. *Phys. Chem. Earth* **2002**, *27*, 1091–1101. [[CrossRef](#)]
17. Rahimi, M.; Hajjam, S.; Khalili, A.; Kamali, G.A.; Stigter, C.J. Risk analysis of first and last frost occurrences in the Central Alborz Region, Iran. *Int. J. Climatol.* **2007**, *27*, 349–356. [[CrossRef](#)]
18. Kalma, J.D.; Laughlin, G.P.; Caprio, J.M.; Hamer, P.J.C. *The Bioclima-Tology of Frost. Its Occurrence, Impact and Protection. Advances in Bioclimatology 2*; Springer: Berlin, Germany, 1992.
19. Crimp, S.; Bakar, K.S.; Kokic, P.; Jin, H.D.; Nicholls, N.; Howden, M. Bayesian space-time model to analyse frost risk for agriculture in Southeast Australia. *Int. J. Climatol.* **2015**, *35*, 2092–2108. [[CrossRef](#)]
20. Hollaway, K. *NVT Victorian Winter Crop Summary 2014*; The State of Victoria Department of Environment and Primary Industry: Brisbane, Australia, 2014.
21. Lush, D. *Queensland 2014 Wheat Varieties*; Grains Research and Development Corporation and the State of Queensland, Department of Agriculture, Fisheries and Forestry: Brisbane, Australia, 2014.
22. Matthews, P.; McCaffery, D.; Jenkins, L. *Winter Crop Variety Sowing Guide 2014*; NSW Department of Primary Industries: Sydney, Australia, 2014.
23. Shackley, B.; Zaicou-Kunesch, C.; Dhammu, H.; Shankar, M.; Amjad, M.; Young, K. *Wheat Variety Guide for Western Australia 2014*; Department of Agriculture and Food, Western Australia: Brisbane, Australia, 2014.
24. Wheeler, B. *Wheat variety sowing guide 2014*. In *South Australia Sowing Guide*; Heaslip, J., Eldredge, L., Treloar, M., Shannon, D., Eds.; SA Grain Industry Trust and Grains Research and Development Corporation: Brisbane, Australia, 2014.
25. Zheng, B.Y.; Chenu, K.; Dreccer, M.F.; Chapman, S.C. Breeding for the future: What are the potential impacts of future frost and heat events on sowing and flowering time requirements for Australian bread wheat (*Triticum aestivium*) varieties? *Glob. Chang. Biol.* **2012**, *18*, 2899–2914. [[CrossRef](#)] [[PubMed](#)]
26. Zheng, B.Y.; Chapman, S.C.; Christopher, J.T.; Frederiks, T.M.; Chenu, K. Frost trends and their estimated impact on yield in the Australian wheat belt. *J. Exp. Bot.* **2015**, *66*, 3611–3623. [[CrossRef](#)] [[PubMed](#)]
27. Potop, V.; Zahranicek, P.; Turkott, L.; Stepanek, P.; Soukup, J. Risk occurrences of damaging frosts during the growing season of vegetables in the Elbe River lowland, the Czech Republic. *Nat. Hazards* **2014**, *71*, 1–19. [[CrossRef](#)]
28. Zhong, X.L.; Wang, D.L.; Zhao, P.; Yan, X.Y.; Su, C.H. Occurrence of frost temperature in Huanghuai wheat production zone after wheat elongation. *Chin. J. Eco-Agric.* **2007**, *15*, 17–20. (In Chinese with English Abstract)
29. Levitt, J. *Response of Plant to Environmental Stress*; Academic Press: London, UK, 1980.
30. Sakai, A.; Larcher, W. *Frost Survival of Plant*; Springer: Berlin/Heidelberg, Germany, 1987.
31. McCarthy, J.J. *Climate Change 2001: Impacts, Adaptation, and Vulnerability: Contribution of Working Group II to the Third Assessment Report of the Intergovernmental Panel on Climate Change*; Cambridge University Press: London, UK, 2001.
32. Cutter, S.L. Vulnerability to environmental hazards. *Prog. Hum. Geogr.* **1996**, *20*, 529–539. [[CrossRef](#)]
33. Brooks, N. Vulnerability, risk and adaptation: A conceptual framework. *Tyndall Cent. Clim. Chang. Res. Work. Pap.* **2003**, *38*, 1–16.

34. Sullivan, C.A. Quantifying water vulnerability: A multi-dimensional approach. *Stoch. Environ. Res. Risk Assess.* **2011**, *25*, 627–640. [[CrossRef](#)]
35. Yue, Y.J.; Li, J.; Ye, X.Y.; Wang, Z.Q.; Zhu, A.X.; Wang, J.A. An EPIC model-based vulnerability assessment of wheat subject to drought. *Nat. Hazards* **2015**, *78*, 1629–1652. [[CrossRef](#)]
36. Blaikie, P.; Cannon, T.D.; Davis, I.I.; Wisner, B. *At Risk: Natural Hazards, People's Vulnerability and Disasters*; Routledge: London, UK, 1994.
37. United Nations International Strategy for Disaster Reduction (UN/ISDR). *Living with Risk. A Global Review of Disaster Reduction Initiatives*; United Nations: Geneva, Switzerland, 2004.
38. Turner, B.L., II; Kasperson, R.E.; Matson, P.A.; McCarthy, J.J.; Corell, R.W.; Christensen, L.; Eckley, N.; Kasperson, J.X.; Luers, A.; Martello, M.L.; et al. A framework for vulnerability analysis in sustainability science. *Proc. Nat. Acad. Sci. USA* **2003**, *100*, 8074–8079. [[CrossRef](#)] [[PubMed](#)]
39. Turner, B.L., II; Matson, P.A.; McCarthy, J.J.; Corell, R.W.; Christensen, L.; Eckley, N.; Hovelsrud-Broda, G.K.; Kasperson, J.X.; Kasperson, R.E.; Luers, A.; et al. Illustrating the coupled human-environment system for vulnerability analysis: Three case studies. *Proc. Nat. Acad. Sci. USA* **2003**, *100*, 8080–8085. [[CrossRef](#)] [[PubMed](#)]
40. Liu, L.; Sha, Y.Z.; Bai, Y.M. Regional distribution of main agrometeorological disaster and disaster mitigation strategies in China. *J. Nat. Disasters* **2003**, *12*, 82–97. (In Chinese with English Abstract)
41. Shi, P.J. *Atlas of Nature Disaster Risk of China*; Science Press: Beijing, China, 2011.
42. Shi, P.J. Natural Disasters in China. In *IHDP/Future Earth-Integrated Risk Governance Project Series*; Jaeger, C., Shi, P.J., Eds.; Springer: Berlin/Heidelberg, Germany, 2016.
43. Zhong, X.; Mei, X.; Li, Y.; Yoshida, H.; Zhao, P.; Wang, X.; Han, L.; Hu, X.; Huang, S.; Huang, J.; et al. Changes in Frost Resistance of Wheat Young Ears with Development During Jointing Stage. *J. Agron. Crop Sci.* **2008**, *194*, 343–349. (In Chinese with English Abstract) [[CrossRef](#)]
44. Feng, Y.X.; He, W.X.; Sun, Z.F.; Zhong, X.L. Climatological study on frost damage of winter wheat in China. *Acta Agron. Sin.* **1999**, *25*, 333–340. (In Chinese with English Abstract)
45. Qi, X.X.; Vitousek, P.M.; Liu, L.M. Provincial food security in China: A quantitative risk assessment based on local food supply and demand trends. *Food Secur.* **2015**, *7*, 621–632. [[CrossRef](#)]
46. Fuller, M.P.; Fuller, A.M.; Kaniouras, S.; Christophers, J.; Fredericks, T. The freezing characteristics of wheat at ear emergence. *Eur. J. Agron.* **2007**, *26*, 435–441. [[CrossRef](#)]
47. Sun, Z.F. *Frost Disasters and Defense Technology*; China Agricultural Science and Technology Press: Beijing, China, 2001; pp. 81–82.
48. Yan, S.Z.; Wang, J.T.; Ran, X.Z.; Wang, Z.T.; Xiao, J.H.; Li, Y.L. The frequency of late frost injury and its preventing method in wheat planted area in Huanghuai. *Meteorol. J. Henan* **2005**, *4*, 40–41. (In Chinese with English Abstract)
49. Liu, J.Y.; Zhuang, D.F.; Zhang, Z.X.; Gao, Z.Q.; Deng, X.Z. The establishment of land-use spatial-temporal database and its relative studies in China. *Geo-Inform. Sci.* **2002**, *3*, 3–7.
50. Liu, J.Y.; Liu, M.L.; Zhuang, D.F.; Zhang, Z.X.; Deng, X.Z. The space analysis of land use pattern change of recent China. *Sci. China (Ser. D)* **2002**, *32*, 1031–1040.
51. Codification Commission of National Atlas. *National Agricultural Atlas of the People's Republic of China*; SinoMaps Press: Beijing, China, 1989.
52. Alexander, D. *Confronting Catastrophe-New Perspectives on Natural Disasters*; Oxford University Press: Oxford, UK, 2000.
53. Crichton, D. *Natural Disaster Management*; Tudor Rose: London, UK, 1999.
54. Dilley, M.; Chen, R.S.; Deichmann, U.; Lerner-Lam, A.L.; Arnold, M.; Agwe, J.; Buys, P.; Kjekstad, O.; Lyon, B.; Yetman, G. *Natural Disaster Hotspots: A Global Risk Analysis*; Disaster Risk Management Series No. 5; The World Bank: Washington, DC, USA, 2005.
55. Wang, L.; Hu, G.F.; Yue, Y.J.; Ye, X.Y.; Li, M.; Zhao, J.T.; Wan, J.H. GIS-based risk assessment of cotton hail disaster and its spatiotemporal evolution in China. *Sustainability* **2016**, *8*, 218. [[CrossRef](#)]
56. Lin, X.M.; Yue, Y.J.; Su, Y. Frost Hazard Risk Assessment of Winter Wheat: Based on the Meteorological Indicator at Different Growing Stages. *J. Catastrophol.* **2009**, *24*, 45–50. (In Chinese with English Abstract)
57. China Meteorological Administration. *Degree of Crop Frost Damage (QX/T 88-2008)*; The National Standard of the People's Republic of China; China Meteorological Administration: Beijing, China, 2008. (In Chinese)

58. Huang, C.F.; Lueng, Y. Estimating the relationship between isoseismal area and earthquake magnitude by hybrid fuzzy-neural-network method. *Fuzzy Sets Syst.* **1999**, *107*, 131–146. [[CrossRef](#)]
59. Huang, C.F.; Moraga, C. A diffusion-neural-network for learning from small samples. *Int. J. Approx. Reason.* **2004**, *35*, 137–161. [[CrossRef](#)]
60. Huang, C.F. Information matrix method for risk analysis of natural disaster. *J. Nat. Disasters* **2006**, *15*, 1–10. (In Chinese with English Abstract)
61. Huang, C.F. *Risk Assessment of Natural Disaster Theory and Practice*; Science Press: Beijing, China, 2005.
62. Xu, L.; Liu, G. The study of a method of regional environmental risk assessment. *J. Environ. Manag.* **2009**, *90*, 3290–3296. [[CrossRef](#)] [[PubMed](#)]
63. Karimi, H.; Saghatoleslami, N.; Rahim, M.R. Prediction of Water Activity Coefficient in TEG-Water System Using Diffusion Neural Network (DNN). *Chem. Biochem. Eng. Q.* **2000**, *24*, 167–176.
64. Zhou, Y.; Yue, Y.J.; Shen, H.; Wang, J.A. Analysis of Wheat Vulnerability to Frost Disaster Based on Hybrid Model of Fuzzy Neural Network. In Proceedings of the 4th Annual Meeting of Risk Analysis Council of China Association for Disaster Prevention, Changchun, China, 16–17 August 2010. (In Chinese with English Abstract)
65. Zhang, X.F.; Ren, Z.H.; Chen, H.L.; Chen, D.; Zou, C.H.; Jin, G.Q. Risk assessment and influence of winter late frost on winter yield. *J. Basic Sci. Eng.* **2006**, *14*, 321–328. (In Chinese with English Abstract)
66. Zhong, X.L.; Wang, D.L.; Li, Y.Z.; Zhao, P.; Yan, X.Y.; Sun, Z.F. Risk assessment of frost damage in wheat. *J. Appl. Meteorol. Sci.* **2007**, *18*, 102–107. (In Chinese with English Abstract)
67. Yu, W.D.; Zhang, X.F. A research on accessing method of frost damage in winter wheat in Huanghai area. *Proc. SPIE Int. Soc. Opt. Eng.* **2009**, 7454. [[CrossRef](#)]



© 2016 by the authors; licensee MDPI, Basel, Switzerland. This article is an open access article distributed under the terms and conditions of the Creative Commons Attribution (CC-BY) license (<http://creativecommons.org/licenses/by/4.0/>).